

OVERCUT AND PROFILE OF THE MACHINED FEATURES IN ELECTROCHEMICAL MACHINING

BISHNU M JHA¹ & A. MANDAL²

¹Centre for Energy Engineering, Central University of Jharkhand, Ranchi, India

²Department of Manufacturing, Engineering, NIFFT, Hatia, Ranchi, India

ABSTRACT

Electrochemical machining (ECM) can be used to machine complex features in hard and difficult to machine materials with negligible tool wear, reasonable accuracy and acceptable surface finish. The accuracy with which the reverse image of the tool is produced in the work piece is of paramount interest in case of ECM. The basic indices that are considered for evaluating the accuracy are the overcut, corner radius and machined profile. In this study two parameters are considered for evaluating the accuracy of machined feature. They are overcut and profile of the shape produced. The first objective is to develop mathematical models based on Box Behnken design to predict the effect of process variables such as applied potential, inter-electrode gap and feed rate on overcut. However overcut alone, gives very limited information regarding the deviation between the tool shape and feature shape produced in the work-piece. To compare the machined and tool profiles, tool and all the machined profiles obtained from experiments are discretized along the perimeter of image and tool, using Analysis™ Five Pro. Software Package Then the variation of energy index (%) is computed using higher order harmonics of elliptic fourier descriptors. The variation in energy index is due to minor undulations in the edges of profile.

KEYWORDS: Box Behnken Design, Denoising, Electrochemical Machining, Machined Features, Overcut, SG Iron, Fourier Descriptors, Profile Analysis

INTRODUCTION

Electrochemical machining (ECM) can be used to machine complex features in hard and difficult to machine materials with negligible tool wear, reasonable accuracy and acceptable surface finish. The material removal rate, accuracy and surface finish depend on many parameters. Only a few of them are controllable. The accuracy with which the reverse image of the tool is produced in the work piece is of paramount interest in case of ECM. The basic indices that are considered for evaluating the accuracy are the overcut, corner radius and machined profile. Over-cut depends on machining voltage, feed rate and electrolyte temperature [1-5]. A higher machining voltage results in higher current density leading to larger over-cut. Higher feed rate reduces over-cut. Temperature of electrolyte affects its conductivity which, in turn, severely affects over-cut. Overcut also depends on type of electrolyte used. Overcut is reported to be higher in case when NaCl is used as electrolyte compared to that when NaNO₃ is used [6].

In this study two parameters are considered for evaluating the accuracy of machined feature. They are overcut, profile of the shape produced. The study is divided into two sections:

- Overcut Analysis &

- Profile Characterization.

Section 1: Overcut Analysis: The objective is to develop mathematical models based on Box Behnken design to predict the effect of process variables such as applied potential, inter-electrode gap and feed rate on overcut. The steps followed are:

- Determining the useful limits of the variables namely feed rate, applied potential, inter electrode gap and electrolytes.
- Selecting the design matrix to conduct the experiments.
- Conducting the experiments as per the design matrix.
- Developing mathematical models based on regression.
- Checking the adequacy of the models.
- Analysis of the results.

1.1 DETERMINING THE USEFUL LIMITS OF VARIABLES

The three controllable ECM parameters selected are applied potential, inter-electrode gap and feed rate. The depth of the shaped hole produced is kept constant i.e. at 2 mm. This step is taken to keep the electrolyte flow pattern more or less uniform for all the experiments. The flow pattern changes significantly as machined depth changes. The useful limits of feed rate, potential and inter electrode gap are chosen based on preliminary experiments conducted and information available in literature. Three electrolytes are chosen namely (a) KCl solution (250 grams/litre of tap water), (b) NaNO₃ solution (400 grams/litre of tap water), (c) KCl + NaNO₃ solution (125 grams of KCl + 250 grams of NaNO₃ /litre of tap water). For simplifying the recording of the conditions of the experiments and processing of the experimental data, the upper, lower and intermediate levels of the variables are coded as +1, -1& 0, respectively by using the following relationship:

$$X_c = \frac{2.0X - 1.0(X_{max} + X_{min})}{(X_{max} - X_{min})} \quad (1)$$

The actual and coded values of the different variables are listed in **Table 1**.

Table 1: Work-Piece Material Specification (SG Iron)

Chemical Composition					BHN	Nodularity*	Matrix
%C	%Si	%Mn	%S	%P			
3.60-3.63	2.30-2.38	0.35-0.36	0.014-0.013	0.083-0.080	179	58.24	Ferritic

1.2 SELECTING THE DESIGN MATRIX

The design matrix is shown in **Table 2**. Electrolyte is not taken as one of the design matrix variable as it is difficult to conduct the experiments in a random order. Hence, three sets of experiments are conducted using the electrolytes to assess their effects on overcuts.

Table 2: The Actual and Coded Values of Different Variables

Variables	Symbol	Low Level		Intermediate Level		High Level	
		Actual	Coded	Actual	Coded	Actual	Coded
Feed Rate (mm/min)	T	0.1	-1.0	0.21	0	0.32	+1.0
Potential (volt)	V	15	-1.0	20	0	25	+1.0
Inter Electrode Gap (mm)	G	0.64	-1.0	0.96	0	1.28	+1.0

1.3 EXPERIMENTATION

For carrying out the experiments ECM machine model ECMAC - II, manufactured by Meta Tech Industries, Pune, is used. Flat hexagon shaped tool made of copper is used. Work-piece material specification is given in **Table 3**.

All the experiments are conducted according to the design matrix but in random fashion to avoid any systematic error creeping into the results. The overcut is defined as the half of the average difference between the opposite sides of the machined feature and the tool. The average distance between the opposite sides of the tool is 18.95 mm.

Table 3: Design Matrix

Sl. No.	Variables		
	F	V	G
1	-1	-1	0
2	+1	-1	0
3	-1	+1	0
4	+1	+1	0
5	-1	0	-1
6	+1	0	-1
7	-1	0	+1
8	+1	0	+1
9	0	-1	-1
10	0	+1	-1
11	0	-1	+1
12	0	+1	+1
13	0	0	0
14	0	0	0
15	0	0	0

1.4 DEVELOPING THE MATHEMATICAL MODEL

To correlate the effects of the variable and overcut the following second order polynomial is selected.

$$Y = B_0 + B_1F + B_2V + B_3G + B_{11}F^2 + B_{22}V^2 + B_{33}G^2 + B_{12}FV + B_{13}FG + B_{23}VG$$

where, B's are the regression coefficients. The controllable ECM parameters F, V, G and their combinations are in coded values.

1.5 CHECKING THE ADEQUACY OF THE MODELS

The analysis of variance (ANOVA) technique [7] is used to check the adequacy of the developed models at 95% confidence level. F-ratios of the models developed are calculated and are compared with the corresponding tabulated values for 95% level of confidence. If the calculated values of F-ratio did not exceed the corresponding tabulated value then the model is considered adequate. The goodness of fit of the models are tested by calculating R^2 , $R^2_{(adjusted)}$ & $R^2_{(predicted)}$.

1.6 RESULTS AND DISCUSSIONS

The coefficients of the models developed and model statistics are given in **Table 4**.

Table 4: The Coefficients of the Models Developed and the Statistical Model Parameters for overcut.

		Overcut, mm			
		Electrolyte	KCl	NaNO ₃	KCl+ NaNO ₃ _1
Coefficients Of The Models Developed	B ₀		1.54419	1.53242	0.75115
	B ₁		-0.07471	-0.20372	-0.08453
	B ₂		0.14525	-0.15517	0.11004
	B ₃		-0.16150	-0.07019	-0.08177
	B ₁₁		0.37022	0.30119	0.33553
	B ₂₂		-0.24580	-0.19912	0.47419
	B ₃₃		-0.44943	-0.30576	0.27196
	B ₁₂		0.15727	0.06000	0.04418
	B ₁₃		0.10373	-0.14442	-0.34117
	B ₂₃		0.11263	-0.05997	0.27195
	F _{RATIO}		0.18844	0.14157	0.29997
	σ ²		0.01651	0.03254	0.03009
	R ²		98.09775	95.18714	96.36034
	R ² _(adj)		94.67370	86.52400	89.80894
	R ² _(pred)		89.95486	77.57353	76.27920

All the models are statistically adequate. Graphs are drawn Figure 1 3 to show how the overcut varies with change in inter electrode gap, applied voltage and feed rate. For the ease of discussion applied potential, inter-electrode gap, feed rate will be referred to as potential, gap, feed rate. The ranges of variation in overcut predicted with KCl, NaNO₃ and KCl+NaNO₃ electrolytes are 0.43 – 2.03, 0.707-2.1 and 0.69 to 1.97 mm respectively. The lower bound of the overcut range predicted with KCl electrolyte is less than that of NaNO₃. The other important trend noticed is that for both KCl and NaNO₃ the maximum is within the design space where as for KCl+NaNO₃_1 the minimum is within the design space. For KCl electrolyte the upper limit of the overcut range decreases as feed rate increases up to a limit and then it starts increasing as feed rate increases further **Figure 1 3**. Similar trends have been observed for both NaNO₃ and KCl+NaNO₃ electrolytes. The overcut range for NaCl+NaNO₃ electrolyte is in-between that of NaCl & NaNO₃ electrolytes. **Table 5** shows the minimum and maximum values of overcut for the three electrolytes.

Table 5: The maximum and Minimum Values of Overcut within a Sphere of Radius $\sqrt{2}$

Electrolyte	Operating Condition for Minimum Overcut				Operating Condition for Maximum Overcut			
	F	V	G	Overcut (mm)	F	V	G	Overcut (mm)
KCl	0.18	-0.96	1	0.449208	-1	-0.1	-0.30	2.03036
NaNO ₃	0.3	1	0.94	0.728875	-1	-0.56	0.18	2.10488
KCl+NaNO ₃	0.44	-0.3	0.58	0.692424	-0.6	1	0.8	1.97034

combination. The active electrolyte and passive electrolytes affect the machining rate and surface finish in more way than one. The concentration of chloride, nitrate anions and their ratios together with current density changes material removal mechanism [9-11]. The range of overcut obtained with KCl+NaNO₃ electrolyte is quite close to that obtained with NaNO₃ electrolyte. This may be due to low chloride to nitrate ratio of 0.5. It is reported that at low current level current density, the current efficiency is very low in case of pure NaNO₃ electrolyte because of oxygen evolution but as the current density increases the current density also increase rapidly [9]. In case of pure NaCl electrolyte current efficiency varies slightly with change in current density and hydrogen evolution takes place at cathode [9]. In case of mixed electrolytes (NaCl + NaNO₃) the current efficiency increases with increase in chloride to nitrate ratio [11].

Section 2: Profile Characterization

One of the major parameters used for measuring the accuracy of feature produced in the work-piece is overcut. However it gives very limited information regarding the deviation between the tool shape and feature shape produced in the work-piece. Shape is very complex to define. In literature shape analysis is broadly classified into two categories (1) External Representation i.e. boundary or edges (2) Internal Representation i.e. region within the external boundary [12]. Some of the thrust areas of shape analysis are shape classification, clustering, character recognition, picture processing and pattern recognition.

Some of the desirable properties of shape representation scheme are uniqueness, invariance under translation, rotation, scaling, reflection, sensitivity: ability to distinguish between similar objects, abstraction from detail: robustness against noise [12]. A large variety of techniques have been developed to analyze shape. Yang Mingqiang et. al. [13] has reported an excellent survey of the important techniques and their relative performance. Fourier Descriptors are widely used shape analysis. The commonly used Fourier Descriptors are complex coordinate [14], elliptic features [15,16] and central distance, curvature function[17], cumulative angle[18]. These descriptors represent the shape of the object. In complex contour representation and scalar contour representation shape signature is obtained. Shape signature is one dimensional representation of a two dimensional outline/ boundary [14]. The low frequency descriptors describe the general features of the shape. The finer details of the object are given by the high frequency descriptors [14]. One of the distinctive features of Elliptic Fourier Descriptors is that geometric interpretation is possible [19].

In elliptic FD, individual work-piece boundary pixels are used to describe the chain code, starting with the upper left pixel of the contour and tracing the boundary clockwise. The chain code enumeration is completed when the original starting point was reached. Using the chain code, a truncated Fourier series expansion of the closed-contour which is a projection on the x and y axes was obtained, given as:

$$x_N(t) = A_0 + \sum_{n=1}^N a_n \cos\left(\frac{2n\pi t}{T}\right) + b_n \sin\left(\frac{2n\pi t}{T}\right) \quad (2)$$

$$y_N(t) = C_0 + \sum_{n=1}^N c_n \cos\left(\frac{2n\pi t}{T}\right) + d_n \sin\left(\frac{2n\pi t}{T}\right) \quad (3)$$

Where t is the step required to traverse 1 pixel along the closed-contour, such that $t_{p-1} < t < t_p$ for code values of p, within the range of $1 \leq p \leq k$ and k is the total number of codes describing the boundary contour. n is the number of Fourier harmonics required to generate the approximation of the boundary (each harmonic has four coefficients). T is the

basic period of the chain code, or steps needed to traverse the entire contour, $T = t_k$. A_0 and C_0 are the bias coefficients, corresponding to a frequency of 0. These coefficients are related to image translation and N is the total number of EF harmonics needed to generate an accurate approximation of the boundary. For each harmonic, the n th set of four harmonic coefficients a_n , b_n , c_n and d_n is defined as:

$$a_n = \frac{T}{2n^2\pi^2} \sum_{p=1}^K \frac{\Delta x_p}{\Delta t_p} \left[\cos\left(\frac{2n\pi t_p}{T}\right) - \cos\left(\frac{2n\pi t_{p-1}}{T}\right) \right], \quad (4)$$

$$b_n = \frac{T}{2n^2\pi^2} \sum_{p=1}^K \frac{\Delta x_p}{\Delta t_p} \left[\sin\left(\frac{2n\pi t_p}{T}\right) - \sin\left(\frac{2n\pi t_{p-1}}{T}\right) \right], \quad (5)$$

$$c_n = \frac{T}{2n^2\pi^2} \sum_{p=1}^K \frac{\Delta y_p}{\Delta t_p} \left[\cos\left(\frac{2n\pi t_p}{T}\right) - \cos\left(\frac{2n\pi t_{p-1}}{T}\right) \right], \quad (6)$$

$$d_n = \frac{T}{2n^2\pi^2} \sum_{p=1}^K \frac{\Delta y_p}{\Delta t_p} \left[\sin\left(\frac{2n\pi t_p}{T}\right) - \sin\left(\frac{2n\pi t_{p-1}}{T}\right) \right], \quad (7)$$

Where t_p is the number of steps required to traverse the first p components or links of the chain code. Δx_p and Δy_p are the spatial changes in the x and y projections of the chain code, respectively, at link p . These values may be 1, 0 or -1 depending on the orientation of link p . Δt_p is the step change required to traverse link p of the chain code.

Equation (6.8) is used to find energy index [20] by finding Fourier power and normalizing it.

$$\text{Fourier power} = \frac{\sum_{n=1}^N (a_n^2 + b_n^2 + c_n^2 + d_n^2)}{2} \quad (8)$$

6.3.1 METHODOLOGY

The profile of the tool is hexagon having 10 mm side. To compare the machined and tool profiles, tool and all the machined profiles obtained from experiments are discretized along the perimeter of image and tool, using AnalysisTM Five Pro. Software Package. The co-ordinates obtained are then used to find the centroid.

6.3.2 RESULTS AND DISCUSSIONS

The coefficients of elliptic FD are calculated. The results for a few selected cases are presented in the **figure 4 7**.

Though, FD is used primarily for shape recognition and shape classification but in this study the objective is to investigate how close the machined profile to the tool profile is. The **Figure 4** shows that with first 14 harmonics the machined profile represents the shape of the tool. The coefficients are all normalized and scale, rotation and translation invariant. **Figure 5a, 6a & 7a** show that more than 99.8% energy index is accounted for by first eight harmonics only. Similar trends are observed for the other machining conditions and electrolytes considered here. So it can be concluded that the machined profile is quite close to the tool profile. The higher frequencies show the finer details. **Figure 5b, 6b & 7b** show the variation of energy index (%) with higher order harmonics. The higher order harmonics account for negligible % of energy index. Here the deviations are in terms of minor undulations in the edges of profile. It may be observed from the

figures that for some case the difference between the two curves are relatively large, for example Figure 6b. From the point of view of good quality of the edge of the profile the minimum difference between work-piece and tool profiles is the best. From the results it may be concluded that machined profile and tool profile are quite close.

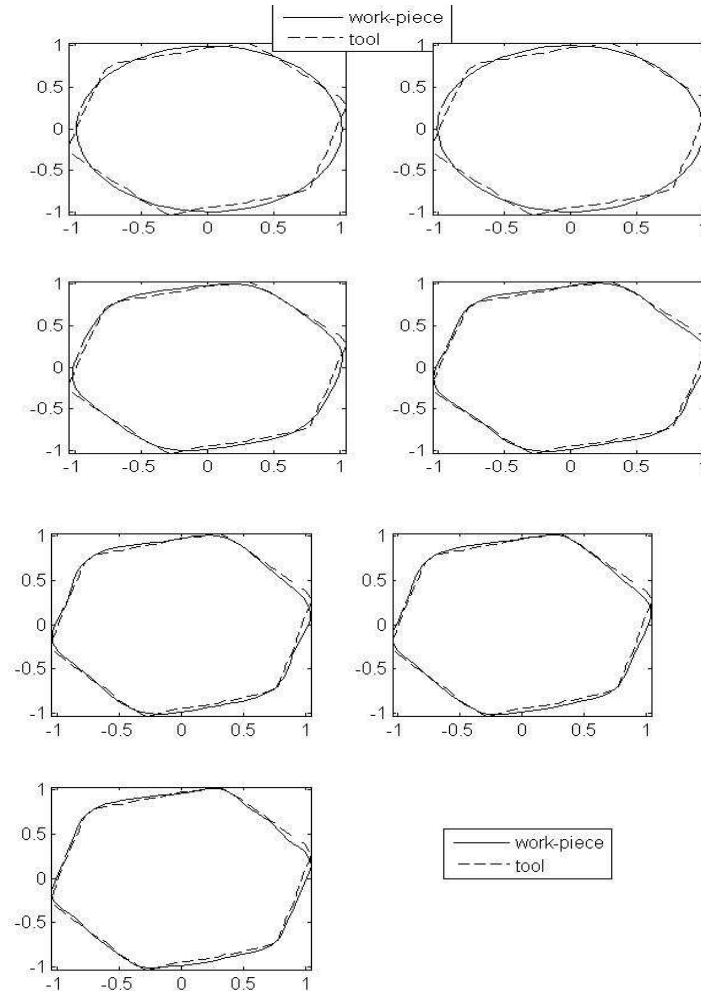


Figure 4: Machined Profile Reconstructed (with a. 2 Harmonics, b. 4 Harmonics, c. 6 Harmonics, d. 8 Harmonics, e. 10 Harmonics, f. 12 Harmonics and g. 14 Harmonics) and Superimposed with Tool Profile..(KCI[-1 -1 0])

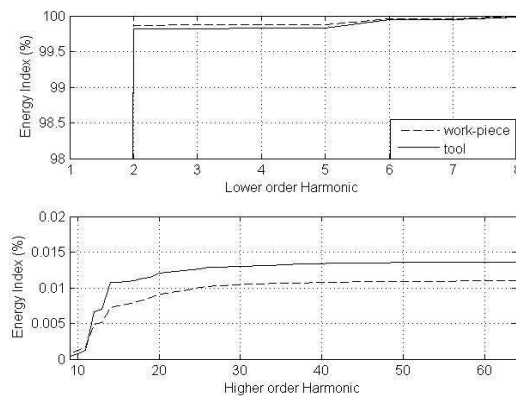


Figure 5: Energy Index for (a. 1-8 Harmonic Components and b. 8-64 Harmonic Components).(KCI[-1 0 1])

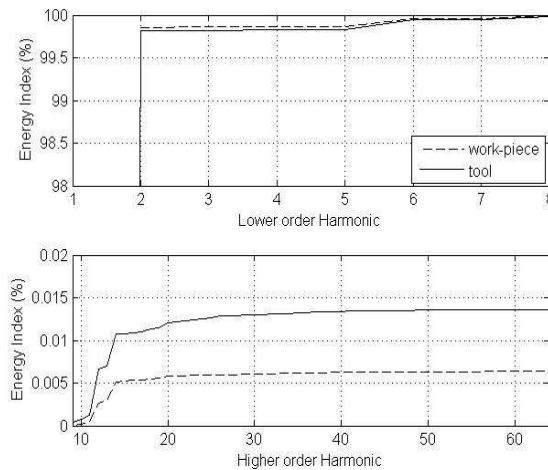


Figure 6: Energy Index for (a. 1-8 Harmonic Components and b. 8-64 Harmonic Components). (NaNO₃[-1 -1 0])

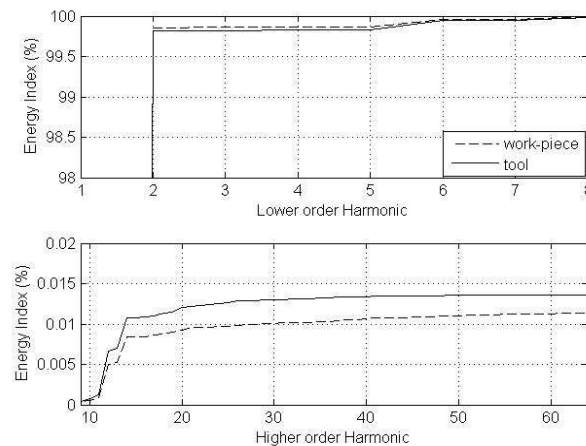


Figure 7: Energy Index for (a. 1-8 Harmonic Components and b. 8-64 Harmonic Components). (NaNO₃+KCl [0 0 0])

CONCLUSIONS

- The ranges of variation in overcut predicted with KCl, NaNO₃ and KCl+NaNO₃ electrolytes are 0.43 – 2.03, 0.707-2.1 and 0.69 to 1.97 mm respectively. The range of overcut obtained with KCl+NaNO₃ electrolyte is quite close to that obtained with NaNO₃ electrolyte. This may be due to low chloride to nitrate ratio of 0.5.
- The variation of overcut with feed rate is nonlinear. The change in overcut is more when feed rate is changed from -1 level to 0/0.5 level compared to that when the feed rate is changed from 0/0.5 to +1 level. However the dominant trend is, as feed increases overcut decreases.
- 99.8% energy index is accounted for by first eight harmonics (of FD) only. So it can be concluded that the machined profile is quite close to the tool profile.
- Higher order harmonics accounts for minor deviations between the tool and machined profile. The smaller the contribution of higher order harmonics better is the quality of machined edges of the profile.

REFERENCES

1. McGeough J.A, Principles of Electrochemical Machining, Chapman and Hall, 1974
2. Rumyantsev E, and Davydov A, Electrochemical Machining of Metals, Mir Publishers Moscow,1989, 13- -36.
3. Ramasawmy H and Blunt L, 3D Surface Topology Assessment of the Effect of Different Electrolytes During Electrochemical Polishing of EDM Surfaces, Int. J. Machine Tools &Manufacture, 2002,vol.42, 567-574.
4. Pa P.S. & Hocheng H., Electro Chemical Machining, Chapter 3 in Advanced Analysis of Nontraditional Machining, Ed. Hocheng H. & Tsai Hung-Yin, Springer, NY, 2013.5. Rajurkar K.P, Schnacker C.L, Lindsay R.P, Some Aspects of ECM Performance and Control, Annals of the CIRP, 1988, vol. 31, no.1, 183-186.
5. João Cirilo da Silva Neto, Evaldo Malaquias da Silva and Marcio Bacci da Silva., Intervening Variables in Electrochemical Machining. Journal of Materials Processing Technology,2006, Vol.179, pp. 92–96.
6. Montgomery D.C., Design and Analysis of Experiments, Ed.5th, Wiley India Pvt. Ltd., N. Delhi, 427,417-419,458-459,448-454.
7. João Cirilo da Silva Neto, Accuracy in Electrochemical Machining: A Study Of Case, 2009, 20th Int. Congress of Mechanical Engineering, Nov. 15 – 20, Gramado, RS, Brazil.
8. Wagner,T., High Rate Electrochemical Dissolution of Iron Based Alloys in NaCl and NaNO₃ Electrolytes. <http://elib.uni-stuttgart.de/opus/volltexte/2003/1293/pdf/TWagDiss.pdf>
9. Lesch A., Wittstock G.,Burger C.,Walther B. and Hackenberg J., External Control of Anodic Mechanism in 100Cr6 Dissolution in Nitrate/ Chloride Mixed Electrolytes, J. Electrochem. Sci. Eng., 2011, vol.1, no.1, 39-54.
10. Mao Kao_Wen and Hoare J.P., The Anodic Dissolution of Mild Steel in Solutions Containing Both Cl⁻ and NO₃⁻ Ions, Corrosion Science, 1973, vol.13, 799-803.
11. Pitas I., Digital Image Processing Algorithms and Applications, 2000, John Wiley and Sons, Canada, 323-382.
12. Yang Mingqiang, Kpalma Kidiyo and Ronsin Joseph, A Survey of Shape Feature Extraction Techniques in Pattern Recognition, Peng- Yang Yin(ed.),2008,43-90.
13. Kauppinen Hannu,Seppanen Tapio and Pietikainen Matti, An Experimental Comparison of Autoregressive and Fourier-based Descriptors in 2D shape classification, IEEE Trans.PAMI-17(2),201-207.
14. Zahn T Charles and Roskies Z Ralph, Fourier Descriptors for Plane Closed Curves, 1972, IEEE Transactions on Computers, vol. C-21, No.3,269-281.
15. Zhang D. and Lu G., A Comparative Study on Shape Retrieval Using Fourier Descriptors With Different Shape Signatures. http://knight.temple.edu/~lakamper/courses/cis601_2008/etc/fourierShape.pdf
16. Xiangyang LI and Yunhe P., Ellipse- Based Description and Retrieval Method, 2002, Science In China (Series F), Vol. 43, no. 4, 299-309.
17. Dengsheng Zhang and Guojun Lu., A Comparative Study on Shape Retrieval Using Fourier Descriptors with Different Shape Signatures.

18. http://knight.temple.edu/~lakamper/courses/cis601_2008/etc/fourierShape.pdf
19. Chung-Lin Huang and Dai-Hwa Huang. A Content-based image retrieval system. 1998, Image and Vision Computing, vol. 16, 149-163.
20. Rochaa, A., Hauagge D.C., Wainer J., Goldenstein S., Automatic fruit and vegetable classification from images, Computers and Electronics in Agriculture, 2010, vol. 70, 96–104.
21. Mebatsion H.K., Paliwal J. and Jayas D.S., Evaluation of Variations In The Grain Types Using Principal Components Analysis of The Elliptic Fourier Descriptors, 2010, Computers and Electronics in Agriculture, 2012, vol. 80, 63-70.

